Supporting Information: Coexistence of Left- and Right-Handed 12/10-Mixed Helices In Cyclically Constrained β-peptides and Directed Formation of Single-Handed Helices upon Site-specific Methylation

Karl N. Blodgett[1], Geunhyuk Jang[2], Sojung Kim[2], Min Kyung Kim[2], Soo Hyuk Choi[2*], and Timothy S. Zwier[1†*]

[1]*Department of Chemistry, Purdue University, West Lafayette, IN 47907-2084 U.S.A.*

[2]*Department of Chemistry, Yonsei University, Seoul 03722, Korea*

Table of Contents

†Present address: Combustion Research Facility, Sandia National Laboratories, Livermore, CA 9455

1. Synthetic Methods and Characterization Data

β-Amino acids (ACHC and 4-methyl-ACHC) and all the β-peptides were synthesized by methods reported previously.[1] 5-Methyl-ACHC was prepared by a method in the following thesis (Kim, S. Handedness Control of Unnatural Peptides with cis-2-Amino-5-methyl-cyclohexanecarboxylic Acid. Master Thesis, Yonsei University: Seoul, Korea, 2018.).

LL-Dimer: ^{1}H-NMR (400MHz, $CDCl_3$) δ 7.53 (d, *J*=9.3 Hz, 1H), 7.37-7.24 (m, 5H), 6.30 (d, *J*=8.2Hz, 1H), 6.18 (t, *J*=5.0Hz, 1H), 4.48-4.31 (m, 3H), 4.06 (m, 1H), 2.59 (m, 1H), 2.37 (dt, *J*=12.3, 3.6 Hz, 1H), 2.04 (s, 3H), 2.00-1.90 (m, 2H), 1.78-1.70 (m, 1H), 1.65-1.24 (m, 11H), 0.96 (d, *J*=6.3Hz, 3H), 0.89 (d, *J*=5.4Hz, 3H); ^{13}C-NMR (100MHz, $CDCl_3$) δ 174.2, 173.2, 169.7, 138.1, 128.7, 127.8, 127.8, 127.5, 49.2, 46.9, 45.8, 43.6, 43.2, 37.0, 32.1, 32.0, 31.6, 30.6, 29.7, 28.8, 28.3, 23.5, 22.7, 22.5, 22.3; MALDI-TOF MS m/z calculated for $C_{25}H_{37}N_3KO_3$ $[M+K]^+$ 466.247, found 466.478.

L-Dimer: ^{1}H-NMR (400MHz, $CDCl_3$) δ 7.39-7.27 (m, 6H), 6.73 (d, *J*=8.1Hz, 1H), 5.96 (t, *J*=5.2Hz, 1H), 4.42 (m, 2H), 4.25 (m, 1H), 4.05 (m, 1H), 2.59 (m, 1H), 2.52 (m, 1H), 2.02-1.12 (m, 22H), 0.89 (d, *J*=6.2Hz, 3H); ^{13}C-NMR (100MHz, $CDCl_3$) δ 173.9, 173.3, 170.0, 132.9, 126.9, 126.5, 126.4, 53.4, 53.0, 45.4, 45.2, 43.9, 30.2, 25.8, 24.4, 24.3, 23.6; MALDI-TOF MS m/z calculated for $C_{24}H_{35}N_3NaO_3$ $[M+Na]^+$ 436.257, found 435.724; calculated for $C_{24}H_{35}N_3KO_3$ $[M+K]^+$ 452.231, found 452.625.

RR-Dimer: ^{1}H-NMR (400MHz, $CDCl_3$) δ 7.38-7.24 (m, 5H), 7.20 (t, *J*=5.2Hz, 1H), 6.10 (d, *J*=9.3Hz, 1H), 6.03 (d, *J*=8.1Hz, 1H), 4.66 (dd, *J*=14.5, 6.8Hz, 1H), 4.24 (dd, *J*=14.8, 5.5Hz, 1H), 4.02 (m, 1H), 3.86 (m, 1H), 2.58 (m, 1H), 2.02-1.90 (m, 2H), 1.97 (s, 3H), 1.84-1.72 (m, 2H), 1.68-1.43 (m, 8H), 1.40-1.18 (m, 3H), 0.93 (m, 6H); ^{13}C-NMR (100MHz, $CDCl_3$) δ 174.0, 172.0, 170.4, 139.6, 128.9, 128.2, 127.6, 48.7, 47.1, 46.0, 43.3, 42.9, 32.2, 31.8, 31.2, 29.8, 29.7, 28.8, 28.5, 23.9, 22.5, 22.3; MALDI-TOF MS m/z calculated for $C_{25}H_{37}N_3KO_3$ $[M+K]^+$ 466.247, found 466.357.

R-Dimer: ^{1}H-NMR (400MHz, $CDCl_3$) δ 7.36-7.23 (m, 6H), 6.77-6.67 (m, 2H), 4.56-4.32 (m, 2H), 4.15-3.92 (m, 2H), 2.65 (m, 1H), 2.26 (m, 1H), 2.15 (s, 1H), 1.98 (s, 3H), 1.82-1.03 (m, 15H), 0.94-0.83 (m, 3H); ^{13}C-NMR (100MHz, CDCl3) δ 174.0, 173.3, 170.4, 137.9, 126.8, 126.5, 126.4, 53.5, 52.9, 45.5, 45.2, 43.9, 30.6, 25.9, 24.8, 24.4, 23.6; MALDI-TOF MS m/z calculated for $C_{24}H_{35}N_3NaO_3$ $[M+Na]^+$ 436.257, found 436.761.

Dimer: ^{1}H-NMR (400MHz, $CDCl_3$) δ 7.43-7.21 (m, 5H), 6.95 (d, J=11.6Hz, 1H), 6.68 (m, 1H), 6.59 (d, J=15.6Hz, 1H), 4.42 (m, 2H), 4.18 (m, 1H), 3.98 (m, 1H), 2.56 (m, 1H), 2.41 (m, 1H), 2.07-0.79 (m, 21H); ^{13}C-NMR (100MHz, CDCl3) δ 174.2, 173.8, 170.4, 133.0, 126.8, 126.5, 53.4, 53.0, 45.5, 45.2, 43.9, 31.2, 25.5, 24.4, 23.3, 23.0; MALDI-TOF MS m/z calculated for $C_{23}H_{33}N_3NaO_3$ $[M+Na]^+$ 422.241, found 422.617.

Trimer: ^{1}H-NMR (400MHz, $CDCl_3$) δ 7.42-7.05 (m, 7H), 6.92 (s, 1H), 6.56 (s, 1H), 4.53-4.30 (m, 2H), 4.28 (m, 1H), 4.17 (m, 1H), 3.93 (m, 1H), 2.65 (m, 1H), 2.55 (m, 1H), 2.18 (m, 1H), 1.99 (s, 3H), 1.94-1.23 (m, 24H); ^{13}C-NMR (100MHz, $CDCl_3$) δ 174.1, 173.7, 173.1, 173.0, 169.9, 138.9, 137.1, 128.8, 128.6, 127.9, 127.6, 127.4, 126.0 77.3, 77.2, 77.0, 76.7, 48.1, 47.9, 47.5, 47.2, 45.8, 45.6, 45.0, 44.6, 43.4, 30.3, 29.8, 29.6, 29.3, 29.2, 26.8, 26.4, 26.2, 25.8, 23.5, 23.4, 22.9, 22.5, 22.2, 21.3, 14.1; MALDI-TOF MS m/z calculated for $C_{30}H_{44}N_4NaO_4$ $[M+Na]^+$ 547.326, found 548.132.

Tetramer: ^{1}H-NMR (400MHz, $CDCl_3$) δ 8.89 (s, 1H), 8.30 (m, 1H), 8.30 (m, 1H), 8.10 (m, 1H), 7.65 (m, 1H), 7.40-7.33 (m, 5H), 6.20 (m, 1H), 5.48 (m, 1H), 4.96 (m, 2H), 4.83-4.03 (m, 4H), 2.75-2.45 (m, 4H), 2.18-2.11 (m, 3H), 1.98-0.86 (m, 32H); ^{13}C-NMR (100MHz, $CDCl_3$) δ 174.4, 174.0, 173.9 173.8, 170.4, 133.0, 128.2, 126.7, 125.2, 75.9, 53.4, 53.0, 45.5, 45.4, 45.2, 43.9, 31.2, 25.5, 24.4, 23.3, 23.0, 22.8, 22.5, 22.1; HRMS m/z calculated for $C_{37}H_{55}N_5O_5$ $[M+Na]^+$ 672.4095, found 672.4097.

Copies of mass spectra

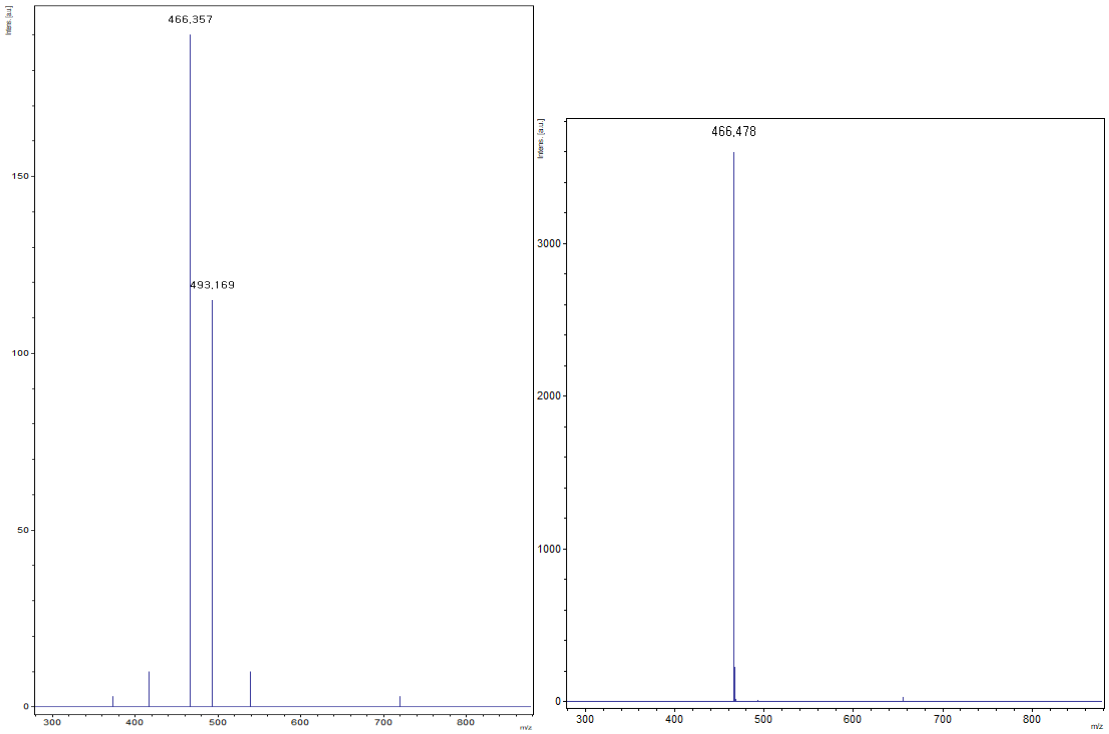

Figure S1: MALDI-TOF mass spectra: LL-Dimer (left) and RR-Dimer (right).

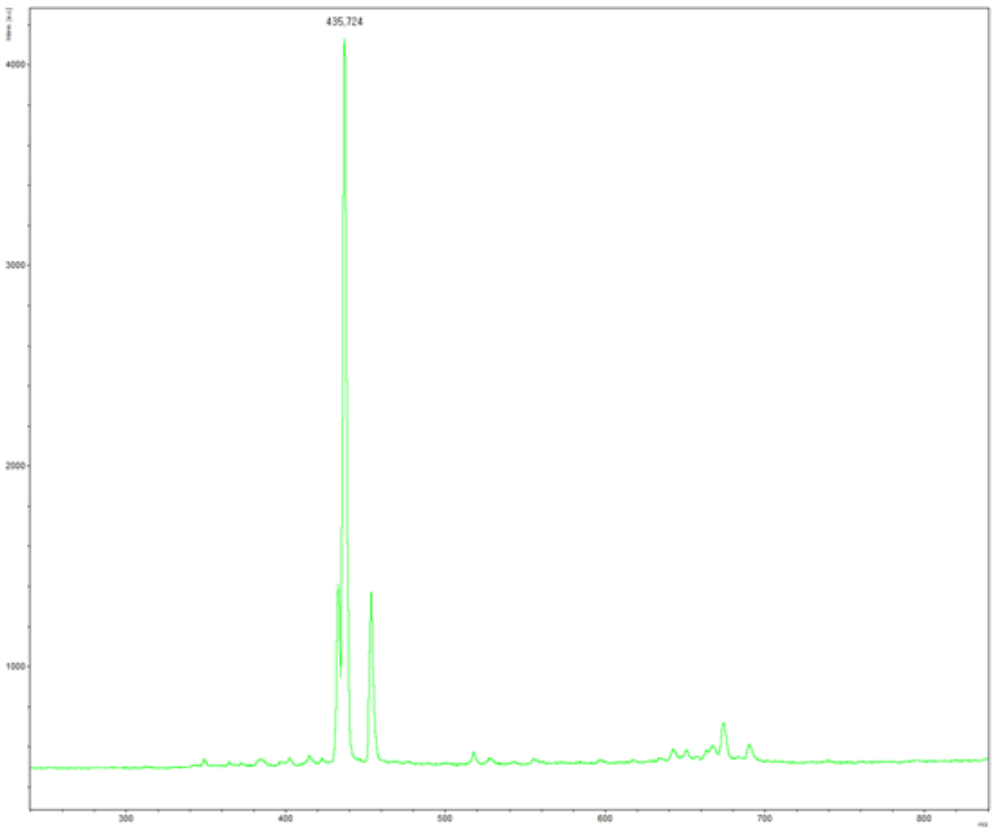

Figure S2: MALDI-TOF mass spectrum of L-Dimer.

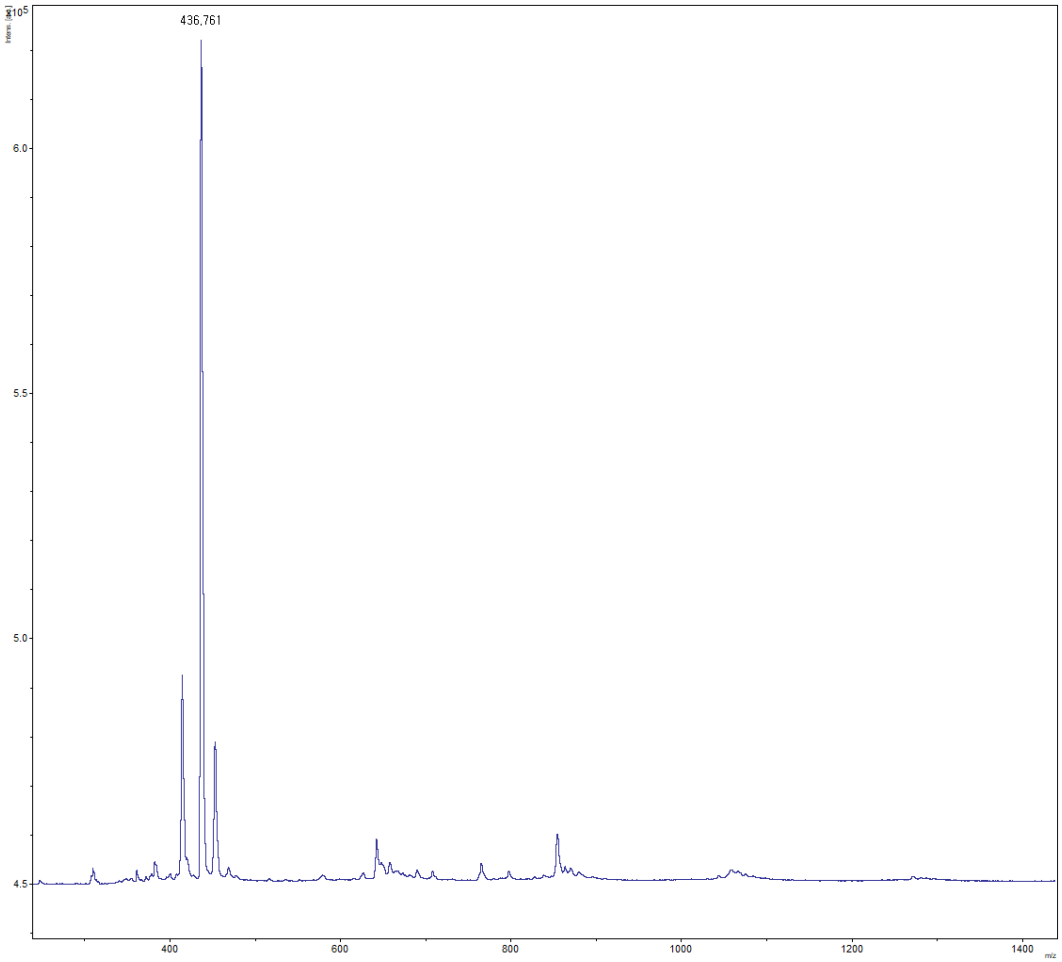

Figure S3: MALDI-TOF mass spectrum of R-Dimer.

Figure S4: MALDI-TOF mass spectrum of Dimer.

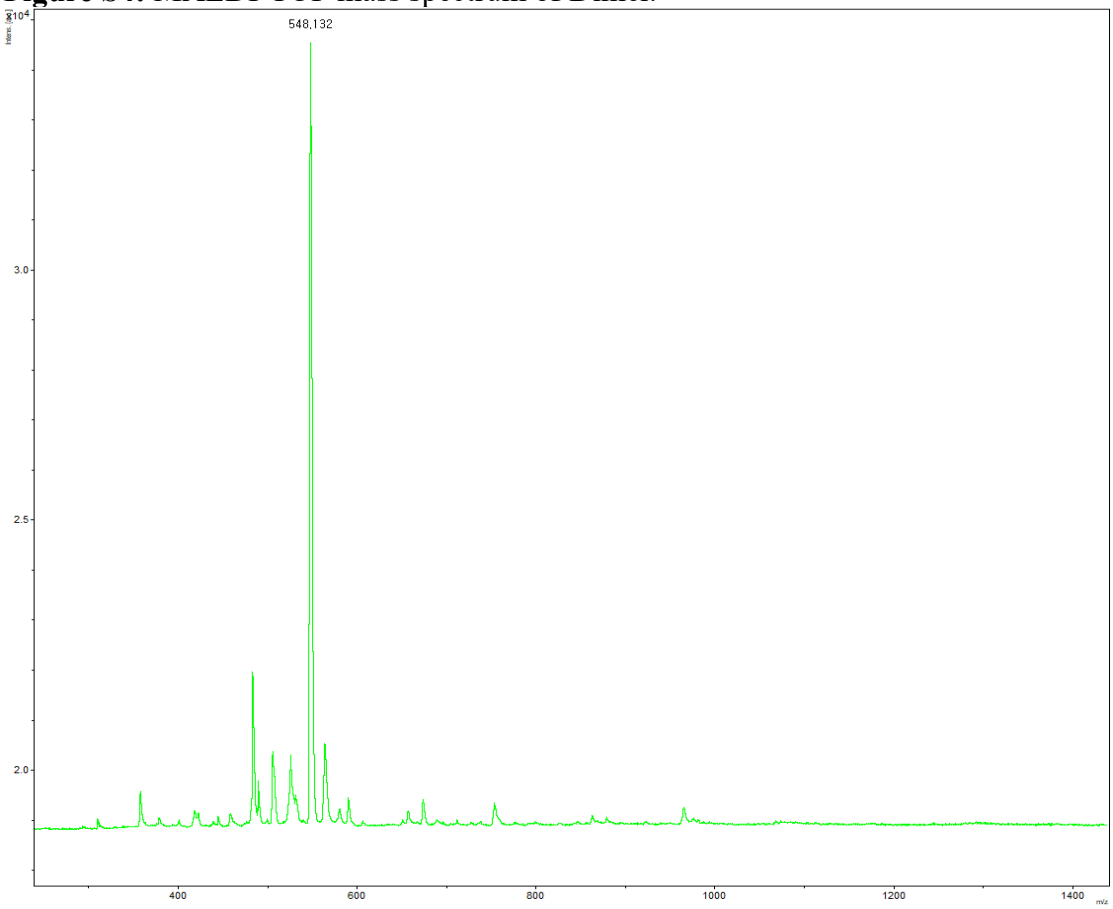

Figure S5: MALDI-TOF mass spectrum of Trimer.

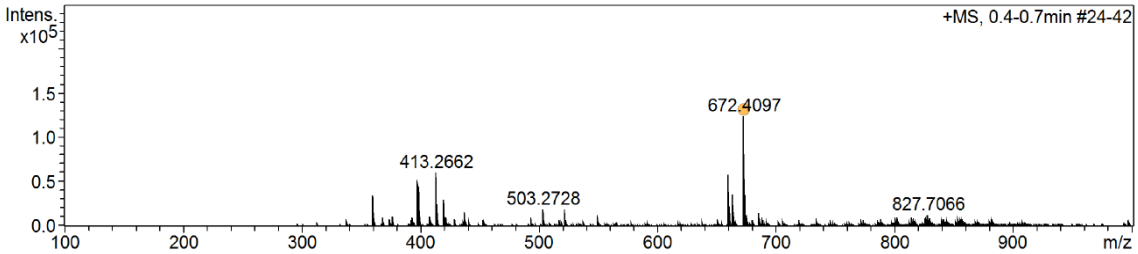

Figure S6: HRMS spectrum of Tetramer.

2. Laser Desorption Details

The solid-state samples were brought into the gas-phase by non-resonant laser desorption from a graphite rod. Aliquots of each sample were crushed to a fine powder and rubbed onto a flat, smooth sanded graphite rod, which is placed directly under the 800 μm nozzle of a pulsed valve (Parker Series 9). The fundamental output of a 20 Hz Nd:YAG laser (Continuum Minilite, 6 ns pulse width, 5 mJ/pulse) is steered to strike the graphite rod surface in a normal orientation, resulting in desorption of the molecules into the gas phase. The pulsed valve is backed with approximately 5.5 bar of Argon gas, which is pulsed into the vacuum chamber at 20 Hz. The desorbed sample is entrained in the supersonic expansion where it is collisionally cooled primarily into the zero-point vibrational level of the lowest energy conformational isomers (conformers) accessible to each molecule. A molecular beam is formed by passing the seeded free expansion through a 3 mm dia. skimmer, where it then enters the ionization region of a Wiley McLaren time-of-flight mass spectrometer, where the cold molecules are probed with UV and IR lasers.

3. UV and IR Spectra of R- and RR-Dimer

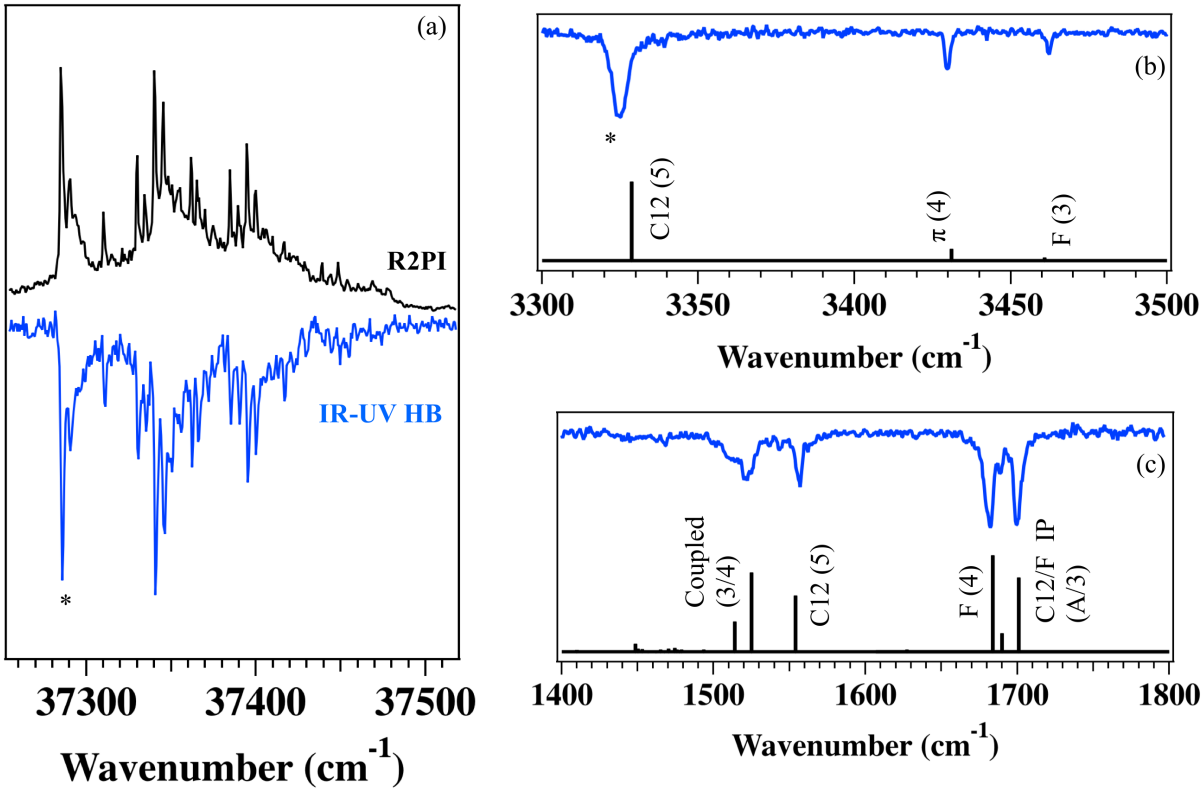

Figure S7: (a) R2PI and IR-UV HB, (b) hydride stretch and (c) amide I and II spectra of the R-Dimer.

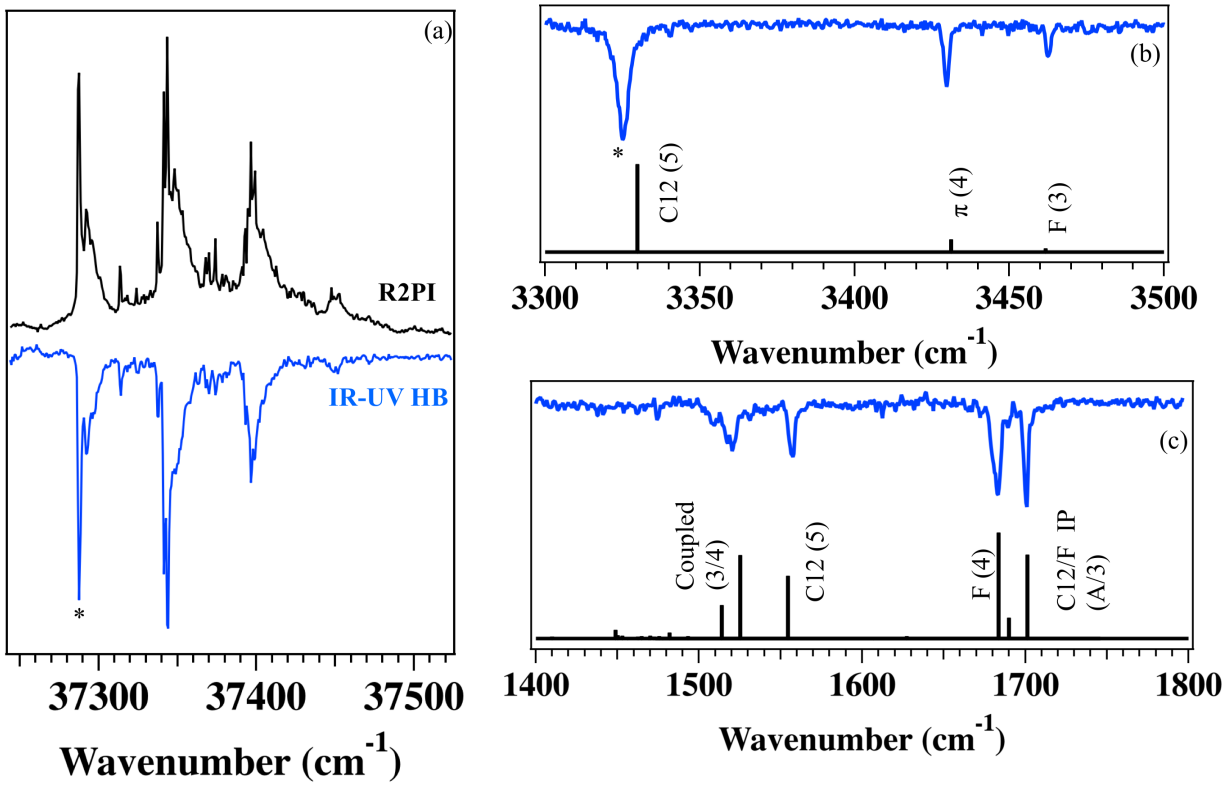

Figure S8: (a) R2PI and IR-UV HB, (b) hydride stretch and (c) amide I and II spectra of the RR-Dimer.

4. Structure and Calculated IR Spectra of Turned Structures at the n=2-4 Level

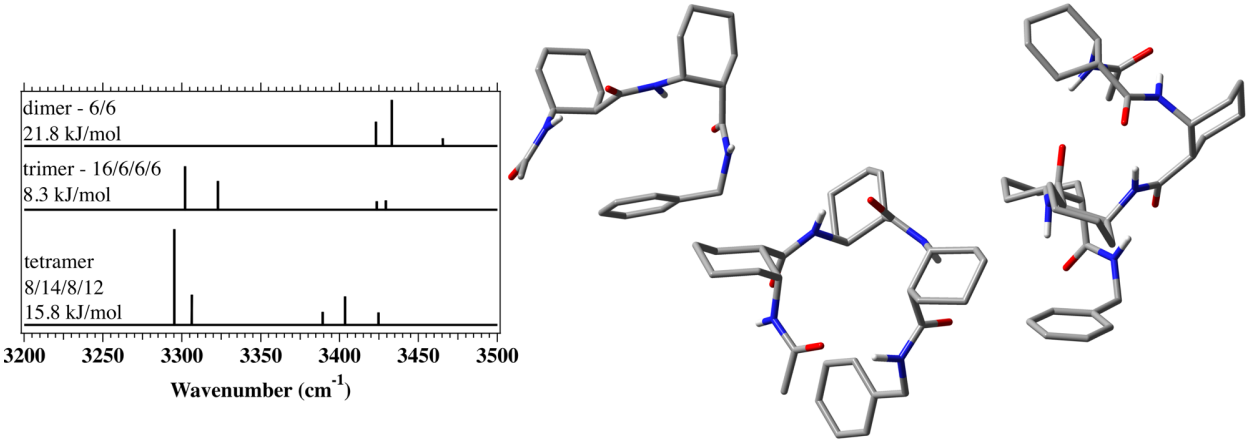

Figure S9: Structure and Calculated IR Spectra of Turned Structures at the n=2-4 Level.

5. UV and IR Spectra of the L-Dimer

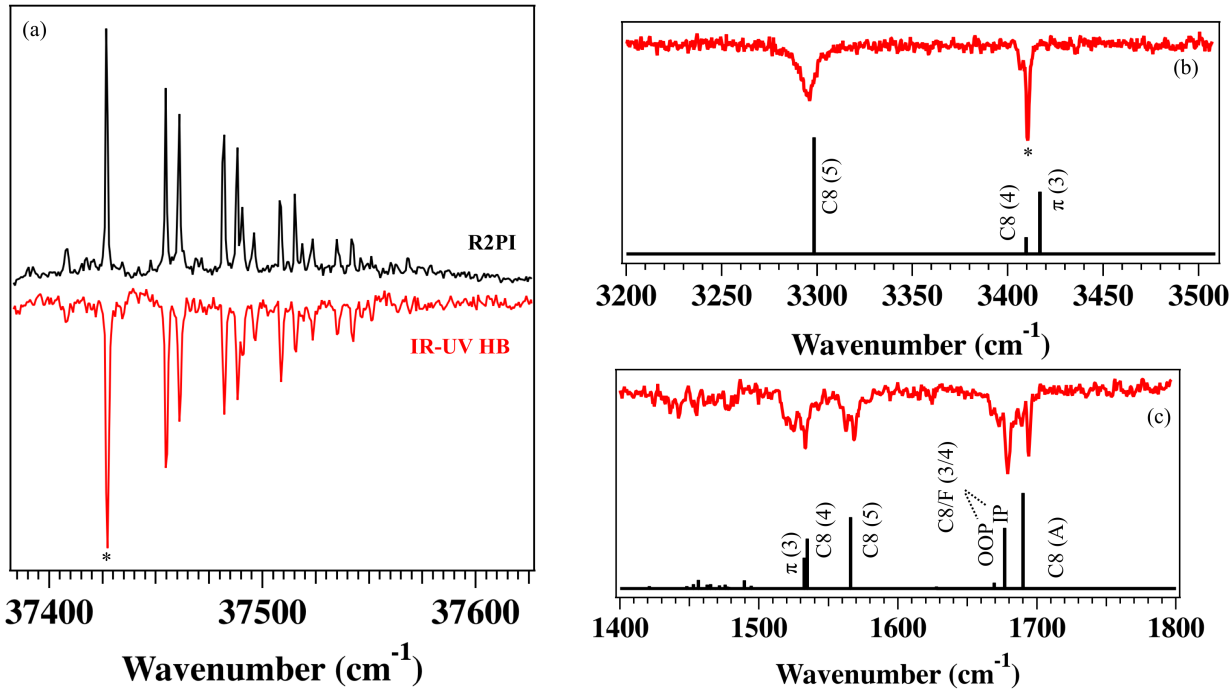

Figure S10: (a) R2PI and IR-UV HB, (b) hydride stretch and (c) amide I and II spectra of the L-Dimer.

6. R2PI Spectra of All Dipeptides

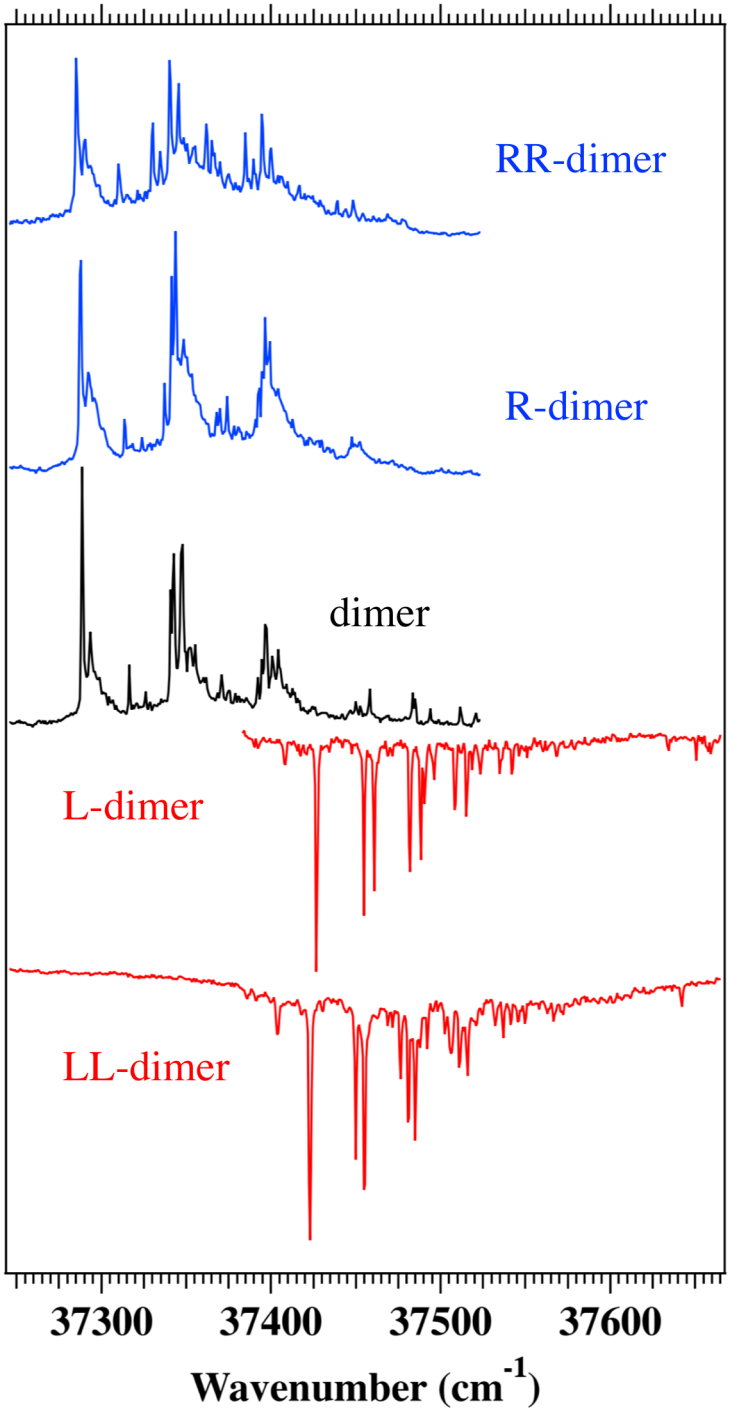

Figure S11: R2PI spectra of all dipeptides studied herein.

7. Calculated IR Spectrum of Trimer Conf B

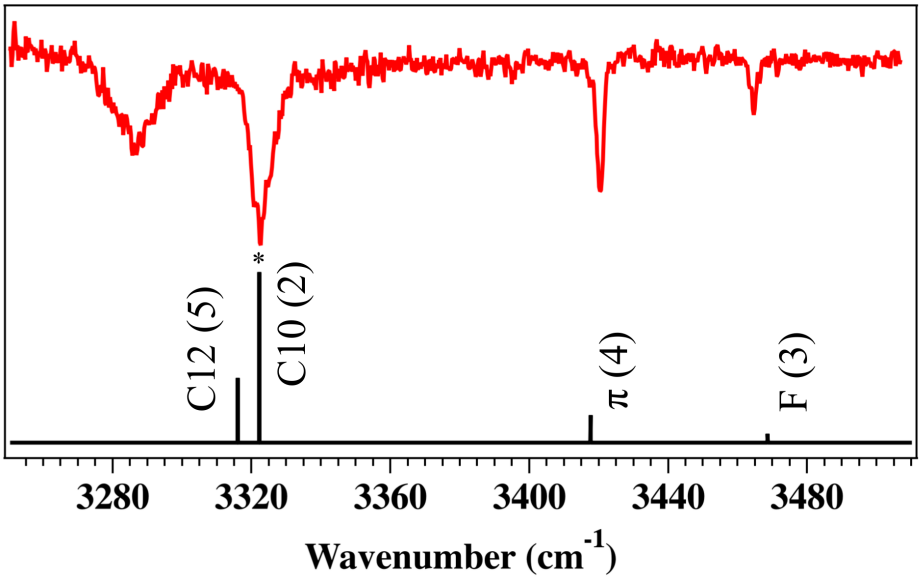

Figure S12: Calculated IR spectrum (black sticks) of Trimer conf B compared with the experimental IR spectrum of Trimer conf A. The peak marked with an asterisk at 3322 cm^{-1} was used to record the IR-UV HB spectrum of conf A, which likely accounts for the contamination from conf B.

8. R2PI Spectra of n=2-4 Main Series Molecules

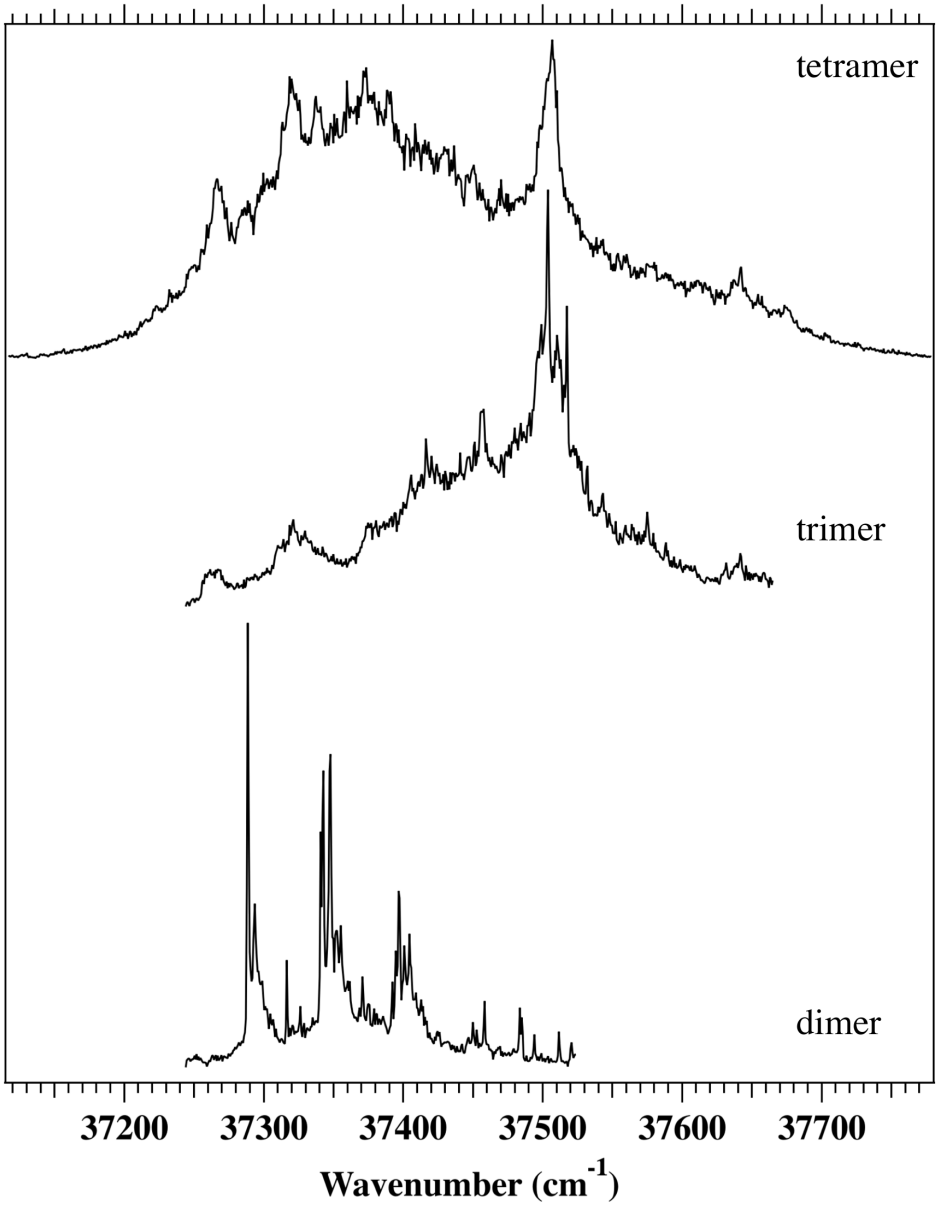

Figure S13: R2PI spectra of n=2-4 main series molecules

9. Calculated IR Spectra of Low-lying Conformers of the Tetramer Compared With Spectrum of Conf A

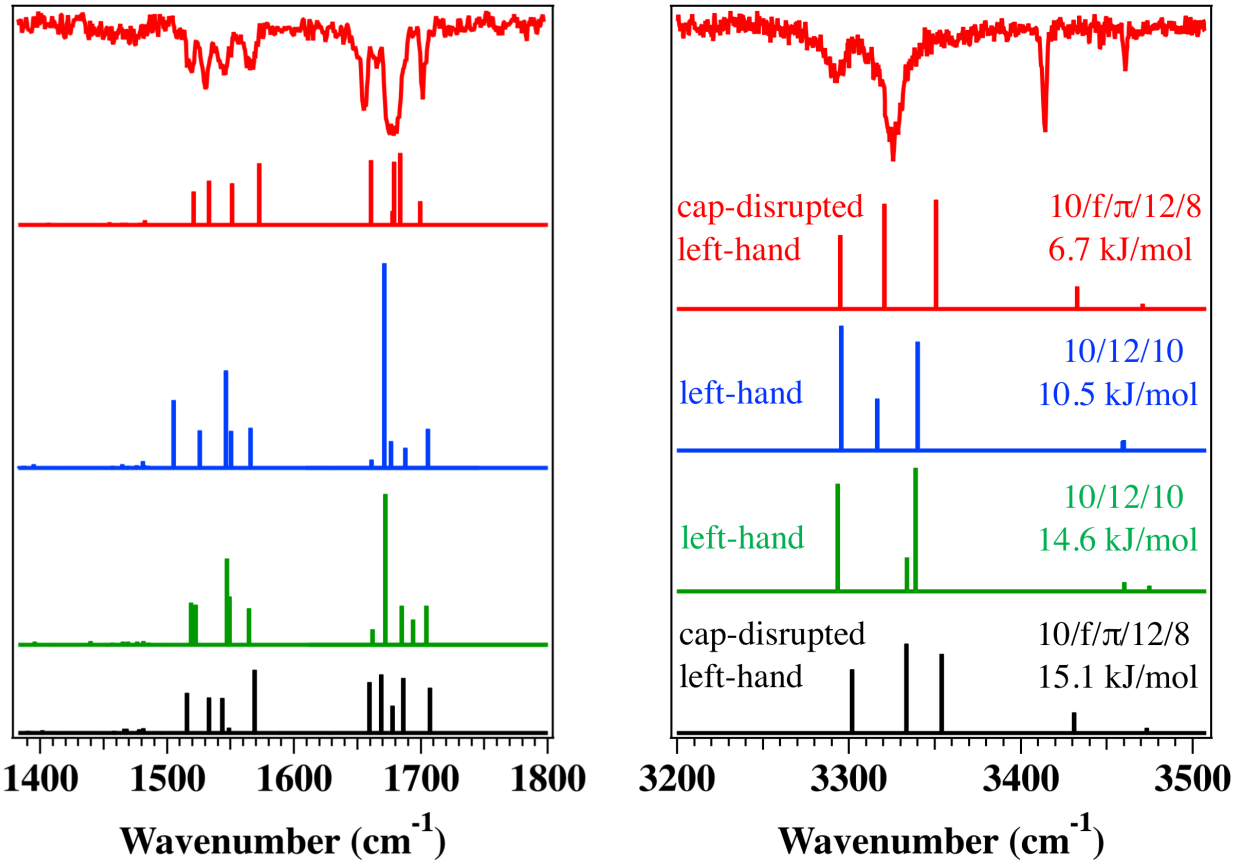

Figure S14: Calculated IR Spectra of low-lying conformers of the tetramer compared with spectrum of conf A in the Amide I/II (left) and NH stretch (right) regions.

10. Free and Potential Energies of All Molecules Studied Herein

Table S1: Relative Energies and Free Energies for structures under 20 kJ/mol of the global energy minimum for the Dimer calculated at the DFT B3LYP-D3BJ/6-31+G(d) level.

Conformer	Structure Type	ΔE (kJ/mol)	ΔG (kJ/mol)
Conf A	R	0	0
AMBER_bp2_cyc_90.log:	L	10.365474	10.459992
AMBER_bp2_cyc_80.log:	R	11.210885	11.2292635
AMBER_bp2_cyc_112.log:	L	11.6230885	11.6230885
AMBER_bp2_cyc_32.log:	L	13.9702855	13.972911
AMBER_bp2_cyc_37.log:	L	14.214457	14.2170825
AMBER_bp2_cyc_31.log:	L	14.4323735	14.4481265
AMBER_bp2_cyc_24.log:	R	16.5065185	16.509144
AMBER_bp2_cyc_109.log:	L	17.43332	17.43332
AMBER_bp2_cyc_85.log:	L	17.968922	17.9820495
AMBER_bp2_cyc_118.log:	L	18.840588	18.8432135

Table S2: Relative Energies and Free Energies for structures under 20 kJ/mol of the global energy minimum for the L-Dimer calculated at the DFT B3LYP-D3BJ/6-31+G(d) level.

Conformer	Structure Type	ΔE (kJ/mol)	ΔG (kJ/mol)
Conf A	L	0	0.462088
NTerm_m__38.log:	R	7.435416	1.62781
NTerm_m__3.log:	L	7.697966	1.9507465
NTerm_m__13.log:	L	8.8243055	6.190929
NTerm_m__40.log:	T	9.1183615	0
NTerm_m__57.log:	R	9.262764	0.8375345
NTerm_m__74.log:	T	10.1055495	3.103341
NTerm_m__15.log:	L	13.8390105	15.8343905
NTerm_m__9.log:	L	16.43563	13.7917515
NTerm_m__19.log:	L	16.5117695	10.2263225
NTerm_m__24.log:	T	17.249535	12.135061
NTerm_m__34.log:	L	17.963671	15.5088285

Table S3: Relative Energies and Free Energies for structures under 20 kJ/mol of the global energy minimum for the LL-Dimer calculated at the DFT B3LYP-D3BJ/6-31+G(d) level.

Conformer	Structure Type	ΔE (kJ/mol)	ΔG (kJ/mol)
Conf A	L	0	0
Nmm__34.log:	L	7.713719	1.1263395
Nmm__10.log:	L	9.042222	5.3901515
Nmm__92.log:	T	17.80089	12.040543
Nmm__11.log:	L	18.3496195	9.730103

Table S4: Relative Energies and Free Energies for structures under 20 kJ/mol of the global energy minimum for the R-Dimer calculated at the DFT B3LYP-D3BJ/6-31+G(d) level.

Conformer	Structure Type	ΔE (kJ/mol)	ΔG (kJ/mol)
Conf A	R	0	0
cTrm_m__30.log:	T	13.2614005	11.016598
cTrm_m__46.log:	R	13.5186995	11.588957
cTrm_m__70.log:	T	14.3273535	14.5741505
cTrm_m__10.log:	L	16.6955545	24.480162
cTrm_m__37.log:	L	16.740188	22.868105
cTrm_m__39.log:	L	17.685368	28.0429655

Table S5: Relative Energies and Free Energies for structures under 20 kJ/mol of the global energy minimum for the RR-Dimer calculated at the DFT B3LYP-D3BJ/6-31+G(d) level.

Conformer	Structure Type	ΔE (kJ/mol)	ΔG (kJ/mol)
Conf A	R	0	0
CTrm_mm__7.log:	L	18.420508	26.7302155
CTrm_mm__30.log:	T	20.667936	21.0486335

Table S6: Relative Energies and Free Energies for structures under 20 kJ/mol of the global energy minimum for the Trimer calculated at the DFT B3LYP-D3BJ/6-31+G(d) level.

Conformer	Structure Type	ΔE (kJ/mol)	ΔG (kJ/mol)
Conf A	L	0	5.1118485
Conf B	R	0.199538	0
TriACHC_5.log:	L	6.768539	3.2897515
TriACHC_40.log:	R	7.6323285	9.1708715
TriACHC_42.log:	T	8.259823	9.6329595
TriACHC_27.log:	R	9.042222	12.0064115
TriACHC_93.log:	L	9.39929	12.240081
TriACHC_24.log:	L	11.5548255	11.8068735
TriACHC_19.log:	L	12.0326665	9.1183615
TriACHC_10.log:	T	13.085492	13.9230265
TriACHC_89.log:	L	15.212147	11.667722
TriACHC_18.log:	L	16.59316	15.9604145
TriACHC_13.log:	R	16.719184	16.813702
TriACHC_44.log:	L	17.6669895	19.607234
TriACHC_20.log:	R	18.2498505	15.926283
TriACHC_55.log:	L	19.2370385	23.204169

Table S7: Relative Energies and Free Energies for structures under 20 kJ/mol of the global [2]energy minimum for the Tetramer calculated at the DFT B3LYP-D3BJ/6-31+G(d) level.

Conformer	Structure Type	ΔE (kJ/mol)	ΔG (kJ/mol)
Conf A	R	0	0
Conf B	L	6.72128	10.3838525
Tetra_53.log:	L	10.5151275	10.55451
Tetra_3.log:	L	14.4901345	17.281041
Tetra_4.log:	L	14.603031	15.1360075
Tetra_7.log:	L	15.12288	18.835337
Tetra_20.log:	L	15.7923825	21.3531915
Am_TetR__10.log:	T	15.8133865	22.742081
Tetra_23.log:	L	16.955479	21.0223785
Tetra_40.log:	L	20.137585	21.6577495

11. Z-Gly$_n$-OH vs Ac-ACHC$_n$-NHBn

A natural point of comparison of the conformational preferences of the present series of molecules is with the aforementioned Z-Gly$_n$-OH, with n=1,3,5. In so doing, we are comparing the least constrained α-peptide ((Gly)$_n$) with a highly-constrained ((ACHC)$_n$) β-peptide in the gas-phase. Interestingly, Z-Gly$_5$-OH adopts an ordered, 14/16 mixed-helix, somewhat analogous to the 12/10 helices studied here. At n=1 and 3 of Z-Gly$_n$-OH, however, the assigned structures shared little H-bonding similarity or dihedral angle patterning with the n=5 14/16 helical motif. This is in sharp contrast to the ACHC series, where even at the dipeptide level the preference for both left- and right-handed mixed helices are apparent (see **Table 1** and **2** of the main text). This fact highlights the role of the ACHC residue as a pre-organized 12/10 helical former.

Furthermore, in the ACHC$_n$ series studied here, all assigned conformers are low-energy structures, in contrast to several other peptides and foldamers studied in the gas-phase where at least one assigned structure is abnormally high in calculated relative energy.[3-7] In these cases, the argument used to explain the presence of such structures is based on entropic grounds, where the temperature behind the expansion nozzle or in the laser-desorption plume renders the entropic term in free energy non-negligible. In such a circumstance, the initial conformational populations are determined not by potential energies, but by the relative free energies, where kinetic trapping and thermodynamic cooling then compete in the expansion process to produce the conformers which are then probed downstream in the molecular beam.

References

1. Jang, G.; Shin, S.; Guzei, I. A.; Jung, S.; Choi, M.-G.; Choi, S. H., Crystal Packing-induced Dimorphism of 12/10-Helical β-Peptides with Dynamic Folding Propensity. *Bull. Korean Chem. Soc.* **2018,** *39* (2), 265-268.
2. Shin, S.; Lee, M.; Guzei, I. A.; Kang, Y. K.; Choi, S. H., 12/10-Helical β-Peptide with Dynamic Folding Propensity: Coexistence of Right-and Left-handed Helices in an Enantiomeric Foldamer. *J. Am. Chem. Soc.* **2016**.
3. Dean, J. C.; Buchanan, E. G.; Zwier, T. S., Mixed 14/16 Helices in the Gas Phase: Conformation-Specific Spectroscopy of Z-(Gly)n, n = 1, 3, 5. *J. Am. Chem. Soc.* **2012,** *134* (41), 17186-17201.
4. Blodgett, K. N.; Zhu, X.; Walsh, P. S.; Sun, D.; Lee, J.; Choi, S. H.; Zwier, T. S., Conformer-Specific and Diastereomer-Specific Spectroscopy of αβα Synthetic Foldamers: Ac–Ala−βACHC–Ala–NHBn. *J. Phys. Chem. A* **2018**.
5. Gord, J. R.; Hewett, D. M.; Hernandez-Castillo, A. O.; Blodgett, K. N.; Rotondaro, M. C.; Varuolo, A.; Kubasik, M. A.; Zwier, T. S., Conformation-Specific Spectroscopy of Capped, Gas-Phase Aib Oligomers: Tests of the Aib Residue as a 310-Helix Former. *PCCP* **2016,** *18* (36), 25512-25527.
6. Gloaguen, E.; De Courcy, B.; Piquemal, J.-P.; Pilmé, J.; Parisel, O.; Pollet, R.; Biswal, H.; Piuzzi, F.; Tardivel, B.; Broquier, M., Gas-phase folding of a two-residue model peptide chain: on the importance of an interplay between experiment and theory. *J. Am. Chem. Soc.* **2010,** *132* (34), 11860-11863.
7. Shubert, V. A.; Baquero, E. E.; Clarkson, J. R.; James III, W. H.; Turk, J. A.; Hare, A. A.; Worrel, K.; Lipton, M. A.; Schofield, D. P.; Jordan, K. D., Entropy-Driven Population Distributions in a Prototypical Molecule with Two Flexible Side Chains: O-(2-Acetamidoethyl)-N-Acetyltyramine. *J. Chem. Phys.* **2007,** *127* (23), 234315.